Computational analysis of stirnol engine

H. Arif

Department of Manufacturing and Engineering Management, National University of Sciences and Technology, Pakistan Navy Engineering College, Karachi, Pakistan,
e-mail: humayun1511@yahoo.com, Tel.: +92-332-5137091

M. Shafique

Department of Aerospace Engineering, Institute of Space Technology, Islamabad, Pakistan.

Received 8 February 2025; accepted 22 October 2025

Global energy requirement is accelerating on daily basis resulting in energy void which leads to human quest to find simple and cost-effective solutions. A promising resolution is the application of renewable energy with thermo-mechanical conversion systems such as Stirling engines. Considerable effort is in hand at industry and academia domains to stimulate the development of Stirling technology. An encouraging answer to this problem is the revival of Stirling engines with the modification of Shape Memory Alloy Nitinol in it. Efficiency of Stirling engine is lower than other Internal Combustion Engines of this class. Stirling engine is being used for power generation but no significant work has been reported on its efficiency improvement; so, the options were required to be explored in order to increase its efficiency. In this regard two dimensions of engineering *i.e.*, Stirling Engine and Shape Memory Alloy were studied and combined. The study employed a two-prong approach, integrating computational modeling and experimental analysis. The results of this integration reveal that addition of Nitinol spring enhances the overall efficiency of engine, demonstrating positive impact of shape memory alloy towards performance output of Stirling engine. The name of newly modified engine is coined as STIRNOL ENGINE (combination of Stirling and Nitinol). This research focuses on modelling of both engines in ANSYS Software and subsequent conduct of computational analysis. The significance of the research is that the low energy wastage (exhausts of home appliances like air conditioners, automobiles, factory waste etc.) can be utilized to run Stirnol engines which can produce useful work.

Keywords: Stirling engine; stirnol engine; nitinol; shape memory effect; low temperature difference engine.

DOI: https://doi.org/10.31349/RevMexFis.72.040601

1. Introduction

Stirling engines have not been utilized and studied to their optimal extent since its inception by Sir Robert Stirling in 1817 [1]. Apart from its disadvantages like very less efficiency, it has many positive aspects like working on a very low temperature gradient. These engines are employed in many practical applications like solar power generation [2,3], cooling microchips [4], providing power to submarines [5], domestic electric facilities and temperature control [6], Stirling engine powered automobiles [7, 8] and Stirling cryocooler [9]. This advantage was focused in the research and an American Stirling Company MM-7 LTD gamma type Stirling engine (Fig. 1) was utilized and modified with a Nitinol spring (a smart material) [10]. The new engine has been named as Stirnol Engine (Fig. 2). In this context, improving Stirling engine efficiency is crucial for recovering low-energy exhaust currently wasted in the atmosphere. By capturing thermal waste from appliances, vehicles, and factories, Stirling engines can harness this energy to produce a functional output. Experimental results revealed that Stirnol engine is slightly more efficient than Stirling engine. This resulted in detailed comparative computational analysis between both engines.

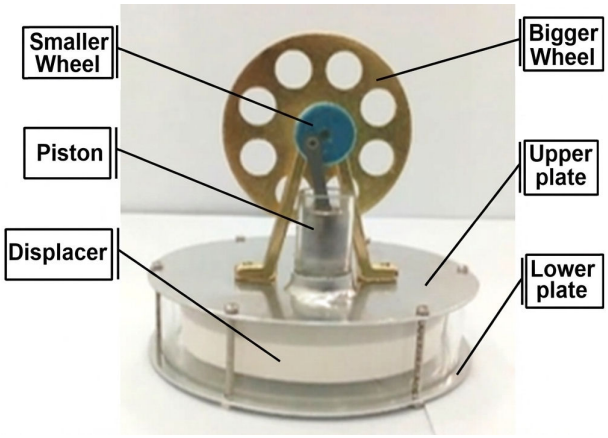

FIGURE 1. Stirling engine.

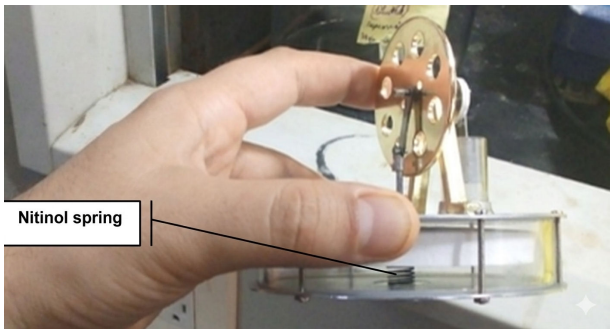

FIGURE 2. Stirnol engine with Nitinol spring.

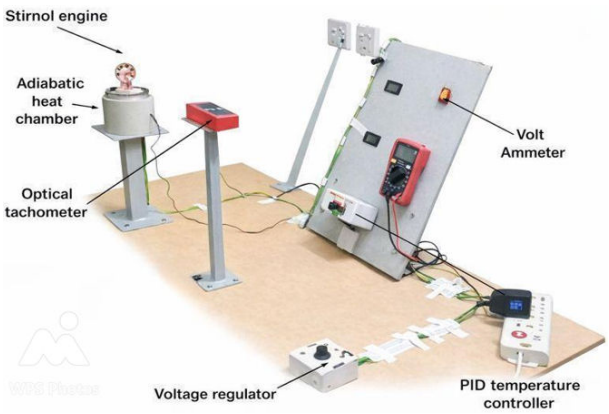

FIGURE 3. Testing facility for Stirling and Stirnol engines.

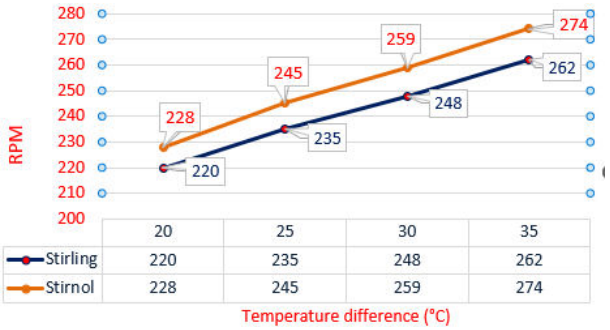

FIGURE 4. Graphical comparison of Temperature difference vs RPM of both engines.

FIGURE 5. Graphical comparison of brake power vs. RPM of both engines.

2. Experimental analysis

Stirnol engine was tested in an experimental setup as shown in Fig. 3. Three parameters were measured and analyzed which were categorized as:

1. Temperature Difference vs Revolutions Per Minute (RPM).
2. Brake Power vs RPM.
3. Eigne Efficiency vs RPM.

All the three categories were studied for both Stirling and Stirnol engines by analyzing them separately in the experimental setup. The results of temperature difference, brake power and engine efficiencies vs RPM are depicted in Table I and Figs. 4, 5 and 6, respectively.

The results were quite encouraging whereby within temperature difference range of $20 - 35°C$, RPM of Stirnol engine was found approximately 10 revolutions more than that of Stirling engine. Brake power of Stirnol engine was found unchanged till 180 RPM and abruptly changed after this value. Between the temperature difference range of $20-35°C$, there was an improved efficiency shown by Stirnol Engine. It was confidently concluded that presence of Nitinol Spring in Low temperature differential Stirnol Engine has improved its efficiency and overall performance [11].

TABLE I. Comparison of Temperature difference vs RPM of both engines.

S. No.	Temp. of upper plate	Temp. of lower plate	Temp. diff ±1	Performance Stirling engine (±1)	Performance Stirnol engine (±1)
		°C		RPM	RPM
1	25	45	20	220	228
2	25	50	25	235	245
3	25	55	30	248	259
4	25	60	35	262	274

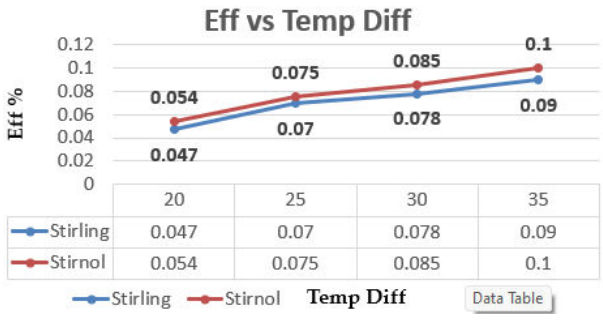

FIGURE 6. Graphical representation of comparative engine efficiencies of Stirling and Stirnol engines at various temperature differences.

3. Computational analysis

Stirling engine has garnered significant attention due to its potential for high energy conversion efficiency and utilization of various heat sources. Computational Fluid Dynamics (CFD) is a powerful software for simulating complex fluid flow and heat transfer phenomena. ANSYS Fluent, a widely-used CFD software, combined with Integrated Computer Engineering and Manufacturing (ICEM) CFD for meshing, offers a comprehensive solution for this problem. The CFD

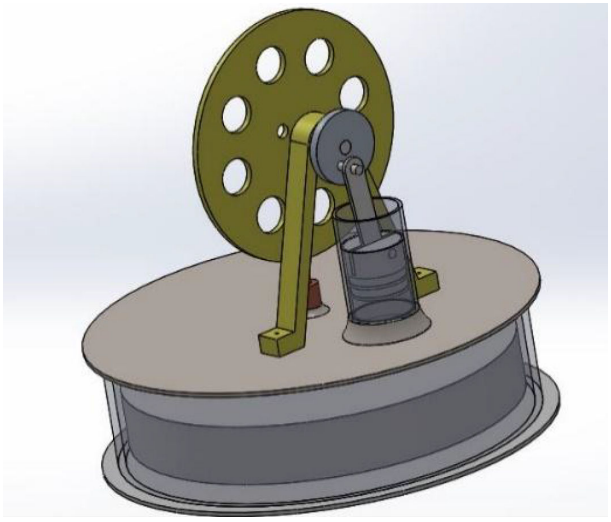

FIGURE 7. Striling engine modeled in ANSYS Software.

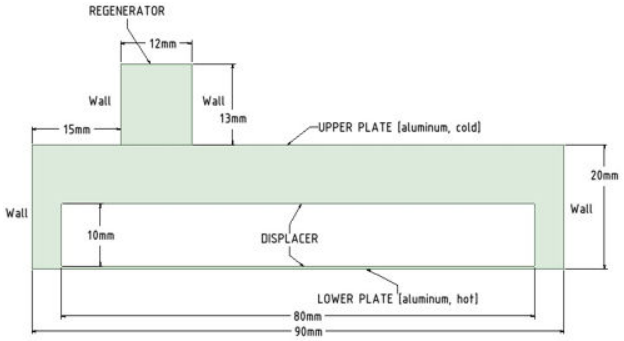

FIGURE 8. 2D CFD Domain.

analysis of Stirling/Stirnol engine aims to study the fluid flow and heat transfer within the engine components, enabling a comprehensive understanding of its performance characteristics. The engine model was constituted in ANSYS software (Fig. 7) and was further approximated using a two-dimensional domain involving piston-cylinder type setup. The CFD domain prepared for the engine is labeled and shown in Fig. 8.

Mesh is created using ICEM CFD software. During the meshing process, careful consideration is given to the different regions of the Stirling engine. For instance, the mesh around the hot and cold cylinders, piston, and heat exchangers is appropriately refined to capture the intricate fluid flow and heat transfer phenomena. Furthermore, mesh quality metrics, such as skewness and aspect ratio, are evaluated and improved to ensure accurate numerical simulations. In addition, four different grids with different mesh sizes were produced by changing the minimum and maximum cell size in

TABLE II. 2D Mesh Characteristics.

S. No.	Description	Value
1	Minimum edge size	0.1 mm
2	Maximum edge size	0.5 mm
3	Maximum skewness	0.64
4	Total number of cells	0.1 million
5	Prism layers	20
6	Prism growth rate	1.2
7	First cell height	0.001 mm

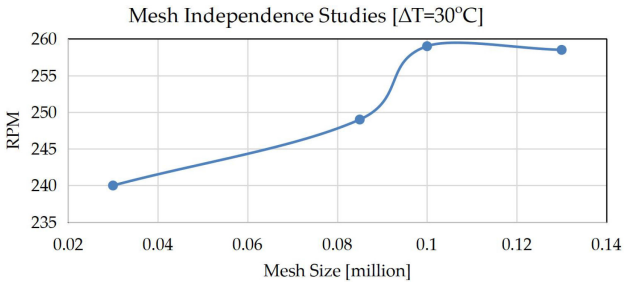

FIGURE 9. Mesh independence studies.

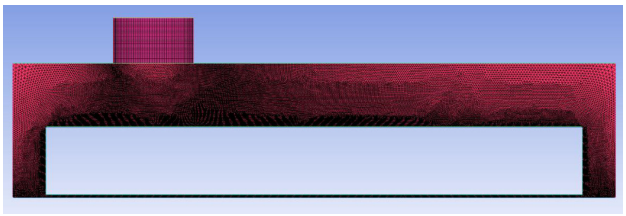

FIGURE 10. Final mesh.

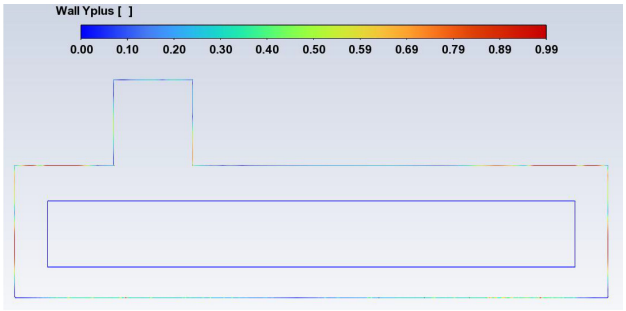

FIGURE 11. Final mesh y+ values.

the domain. The details regarding these meshes and results computed for RPMs developed in the engine are shown in Fig. 9. These mesh independence studies were done at temperature difference of 30°C between the hot and cold plates. Mesh size of 0.1 million was selected as the final mesh. The final mesh characteristics are presented in Table II and the view of mesh is presented in Fig. 10. To capture boundary layer effects accurately within the engine it was desired to keep y+ value within the range of 0-1. The y+ values for the final mesh is shown in Fig. 11. After the meshing process is complete, the model is exported to ANSYS Fluent for two-dimensional analysis.

ANSYS Fluent provides a comprehensive range of options and solvers to simulate fluid flow, heat transfer, and other related phenomena within the Stirnol engine. To capture the exact flow phenomenon inside the engine, appropriate boundary conditions and solver settings need to be defined. This includes specifying the working fluid properties, inlet and outlet conditions, boundary wall conditions and any additional feature unique to the Stirnol engine configuration being analyzed. The temperature values provided in experimental results are used as boundary conditions for lower and upper plates. The working fluid is taken as compressible ideal gas air. The solver settings involve choosing the appropriate numerical schemes for discretization, convergence criteria, time-step size and turbulence models. The choice of turbulence models depends on the flow regime and the level of turbulence present within the Stirling engine. SST K-w turbulence model was used to accurately capture the near wall turbulence effects. Displacer and piston were modeled as moving walls. Smoothing, layering and re-meshing methods available in fluent dynamic mesh settings were used to model the motion of displacer and piston using User Defined Functions (UDF). The results obtained from the analysis can be used to evaluate the performance of Stirling engine, including the efficiency, power output, heat transfer characteristics, and potential areas for improvement. Additionally, sensitivity analyses can be performed by varying parameters such as regenerator design, working fluid properties and operating conditions to understand their impact on the engine performance. The boundary conditions and other CFD analysis properties are summarized in Table III.

3.1. User Defined Function

User defined function (UDF) is a tool in ANSYS fluent to model custom motion for moving boundary in a computational domain for transient analysis. To model the motion of displacer and piston a GRID_MOTION UDF is created in C

TABLE III. Boundary conditions for CFD analysis.

S. No.	Parameter	Boundary condition
1	Turbulence model	SST K-w
2	Time step	0.0005 seconds
3	Steady iterations per time step	20
4	Numerical scheme	Coupled
5	Pressure, density, energy formulation	Second order
6	Moving and stationary walls	No-slip
7	Hot and cold plate	Constant temperature stationary wall
8	Working fluid	Fixed volume air with ideal gas law

language and imported in FLUENT to conduct the dynamic mesh transient analysis of Stirling and Stirnol engines. To model the motion of displacer and piston in UDF, following equations are used as motion models:

$$Y_{\text{displacer}} = Y_{d0} + A_d \sin\left(2\pi\frac{RPM}{60}t + \frac{\pi}{2}\right), \quad (1)$$

$$Y_{\text{piston}} = Y_{r0} + A_r \sin\left(2\pi\frac{RPM}{60}t\right), \quad (2)$$

where $Y_{\text{displacer}}$ and Y_{piston} is the displacement of displacer and piston in y-axis, Y_{d0} and Y_{r0} are the initial position of displacer and piston, A_d and A_r is the amplitude of displacement of the displacer and piston, RPM is the engine speed in revolution per minute and "t" is the time in seconds. The above-mentioned equations are for the Stirling engine. To model the Stirnol engine slight modification in the equations is required to model the effect of Nitinol spring. Following equations are used to model the effect of Nitinol spring in Stirnol engine.

$$Y_{\text{displacer}} = Y_{d0} + A_d \sin\left(2\pi\frac{RPM}{60}t + \frac{\pi}{2}\right) + A_s \sin\left(\sqrt{\frac{K}{m}}t\right), \quad (3)$$

$$Y_{\text{piston}} = Y_{r0} + A_r \sin\left(2\pi\frac{RPM}{60}t\right) + A_s \sin\left(\sqrt{\frac{K}{m}}t\right), \quad (4)$$

where A_s and m is the length of Nitinol spring and mass of displacer respectively. K is the martensite phase spring constant of Nitinol spring.

Figure 12 shows the displacement of piston and displacer w.r.t time during one engine cycle. The graph shows that the motion of displacer and piston has a phase shift of 90° throughout the working of the engine. Figure 13 shows the work done vs time graph of Stirling and Stirnol engines as

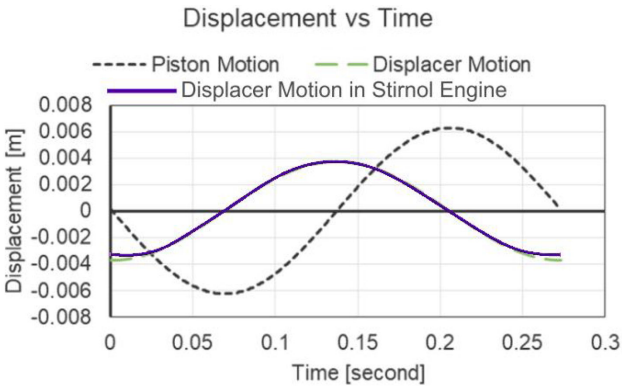

FIGURE 12. CFD-Position of displacer and piston with time during one engine cycle.

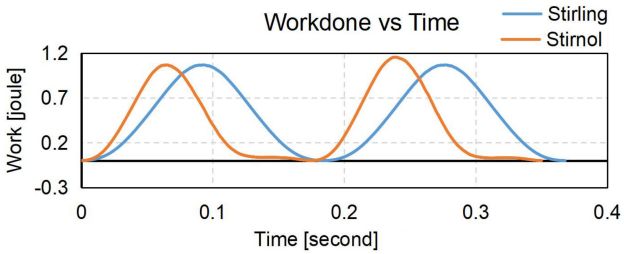

FIGURE 13. Work time chart of Stirling engine.

TABLE IV. Condition for CFD analysis of Stirnol engine.

S. No.	Parameters	Values			
1	ΔT between hot & cold plates	20 K	25 K	30 K	35 K
2	Engine RPM (± 1)	228	245	259	274

computed from CFD for two revolutions of engine wheel. A sinusoidal pattern in force generation is experienced which means that as the displacer come down towards hot plate the air compresses and exerts a force on displacer.

This exerted force will have a highest magnitude when the displacer is at its bottom most position. As the displacer starts moving up, the force generated is reduced until the displacer reaches its top most position. The conditions used for CFD analysis are presented in Table IV.

4. Results and discussions

The CFD analysis was performed for 6 seconds engine operation with the conditions provided in Table IV. The results obtained were post processed in ANSYS fluent and CFD-Post tools. Figure 14 shows complete engine cycle with temperature distribution in displacer and piston cylinders at each phase of engine cycle. It can be seen that the air is expanding from phase 1 to phase 2 due to heat addition from base plate and the volume of air increases between displacer and base plate. This heat addition continues from phase 2 to phase 3 with constant volume. From phase 3 to phase 4 the heat addition continues; however, due to the displacer motion towards base plate the air between displacer and base plate undergoes compression and the volume of air between base plate and displacer decreases. This compression increases the pressure of air. The pressure of air between displacer and base plate increases further due to increase in temperature from phase 4 to phase 1, however the volume remains fixed because the displacer cannot go further down due to the mechanical constraints and Nitinol spring compression limit. This completes one engine cycle and the pattern is repeated in all other engine cycles.

The work done by engine in one engine cycle is equal to the average force on displacer during one engine cycle multiplied by the total distance covered by the displacer in its

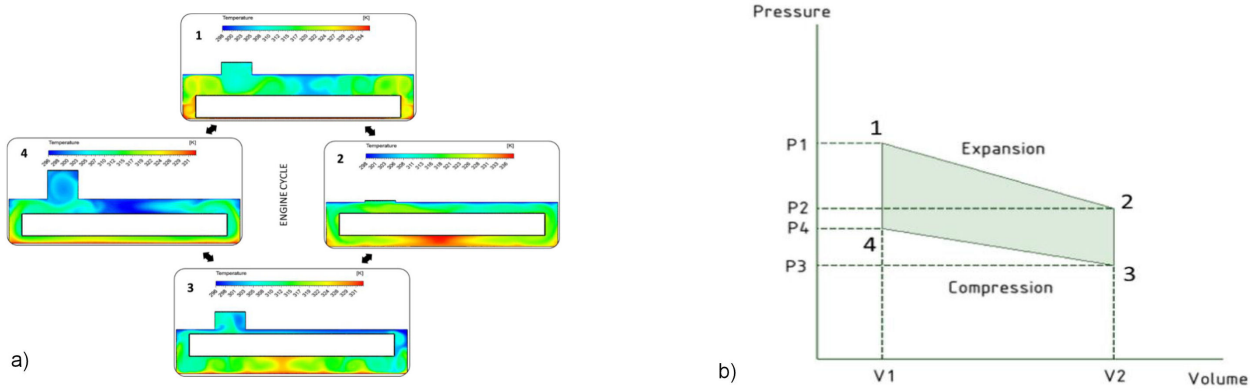

FIGURE 14. Engine cycle of Stirnol engine.

journey during one engine cycle. In Fig. 14, the displacer compresses the Nitinol spring from phase 4 to phase 1. This compression increases the potential energy of Nitinol spring. The potential energy of Nitinol spring further increases at phase 1 due to the heat addition by base plate. This heat addition due to conduction is dependent on the material of base plate. For materials whose thermal conductivity is higher, the heat addition to Nitinol spring would be higher. However, in this CFD analysis thermal conduction is not modeled to keep the transient analysis simple and efficient; therefore, the increase in Nitinol spring potential energy due to conduction at phase 1 is modeled using user defined functions. The conduction further increases the potential energy of Nitinol spring which is then utilized as work when the displacer starts moving up from phase 1 to phase 2. This scheme is numerically demonstrated in equations below. The increase in potential energy of Nitinol spring is converted to increase the potential energy of working fluid which can be seen in Fig. 15. This change produced in the potential energy of Nitinol spring at phase 1 increases the efficiency and power of Stirnol engine.

Phase 4: Potential energy of Nitinol spring $= P_o$

Phase 4 to Phase 1: Potential energy of Nitinol spring $= P_o + P_{\text{compression}}$

Phase 1: Potential energy of Nitinol spring $= P_o + P_{\text{compression}} + P_{\text{conduction}}$

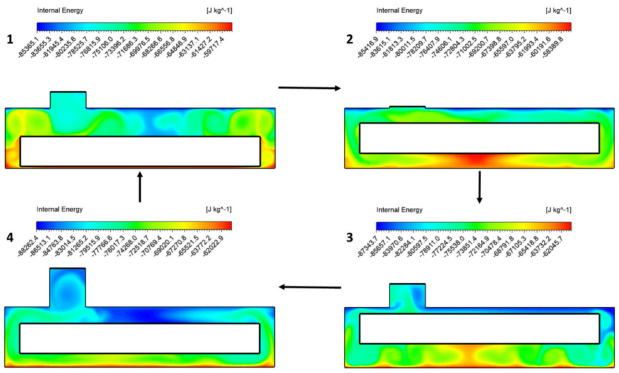

FIGURE 15. Internal energy of working fluid during one engine cycle of Stirnol engine.

It is worth observing that during each engine cycle, an increase in temperature would result in increased internal energy in displacer and piston cylinder. For a real engine, all the properties of the working fluid are interlinked; hence, whenever the compression of working fluid occurs the pressure, density and temperature of the working fluid increases. Whenever, the working fluid undergoes expansion, its volume would increase to obey ideal gas law. These aspects can be observed in Figs. 16 and 17. Another important phenomenon is that of viscosity and skin friction. The motion of piston and displacer transfer their motion to particles of working fluid. This motion of working fluid particles generates motion patterns or velocity in working fluid in the form of circulation. The circulation in the working fluid would increase as the RPM of the engine increases. The velocity in working fluid increases the heat transfer from base plate to working fluid through convection and it can be deduced that higher the RPM, higher will be the convection rate; however, there is a limit to this convection rate. There will be a specific RPM after which if the RPM of engine is increased the convection rate would not increase further or the rate of increase in convection would drop considerably and the efficiency of engine would drop.

In addition to the increase in heat transfer through convection, the velocity of working fluid would create viscous

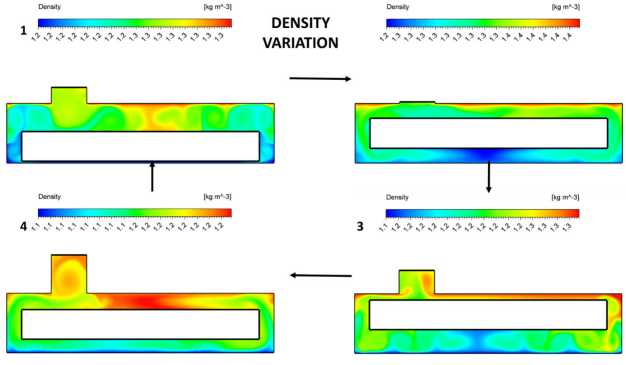

FIGURE 16. Density variation in one engine cycle of Stirnol engine.

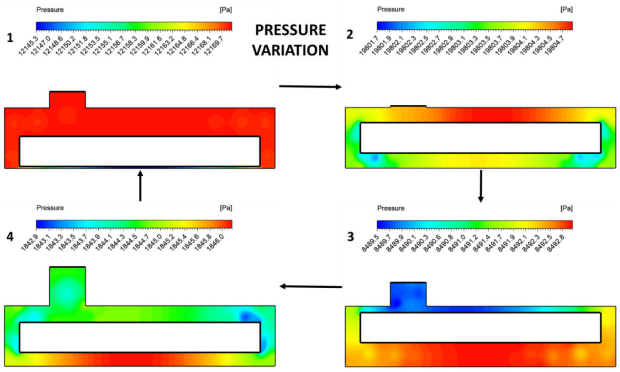

FIGURE 17. Pressure variation in one engine cycle of Stirnol engine.

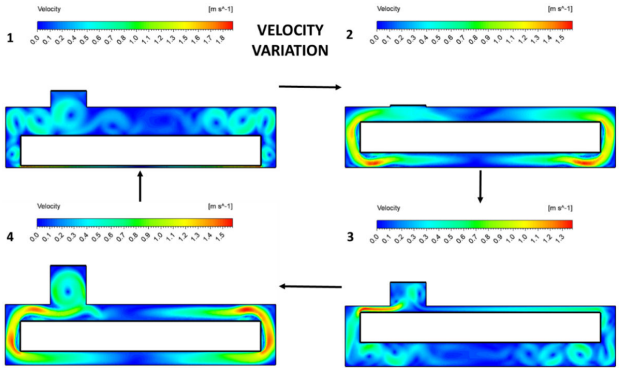

FIGURE 18. Velocity variation in working fluid during one engine cycle of Stirnol engine.

effects on the displacer. Higher the velocity of the working fluid, higher will be the viscous effects. As the RPM of engine increases, more velocity would be created in working fluid and the viscous effects or skin friction on displacer would increase. As a result, more energy would be required for the displacer to continue its motion. In other words, these viscous effects would not only consume the energy transferred to displacer during engine cycle but also decrease the power output and efficiency of the engine. Figure 18 depicts this phenomenon in the form of velocity variation in working fluid during one complete engine cycle.

The CFD simulations for Stirnol engine were performed for all the condition mentioned in Table IV and the post processing for pressure, temperature, density, velocity and internal energy variation in the working fluid are shown in Figs. 14-18. Table V shows the summary of computed average power and efficiency of Stirnol engine from one cycle of engine run in CFD.

TABLE V. CFD: Average power and efficiency of stirnol engine.

S. No.	Parameter	Values			
1	ΔT [K]	20	25	30	35
2	RPM ($\pm$1)	228	245	259	274
3	Average Power [mW]	2.97	3.16	3.21	3.52
4	Efficiency [%]	0.064	0.073	0.091	0.105

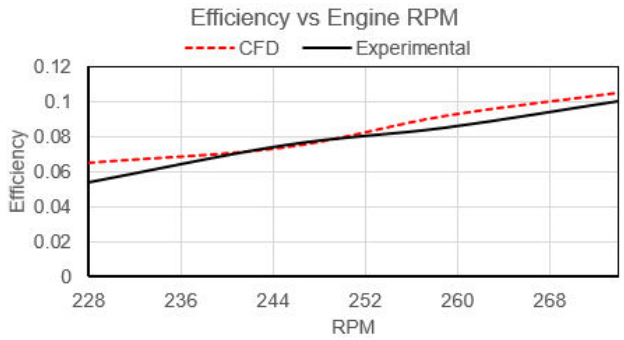

FIGURE 19. Efficiency of Stirnol engine calculated from CFD.

$$\eta = \frac{W_{\text{avg}}}{Q_{\text{in}}}, \tag{5}$$

where η is the efficiency, W_{avg} is the average work done by the displacer in one engine cycle, and Q_{in} is the total heat energy provided to the engine during one cycle.

The efficiency of the engine is calculated using the average work done by displacer in one engine cycle divided by the total heat energy provided to the engine during one engine cycle. The efficiency calculated from CFD is then compared with the efficiency calculated from experimental work. Figure 19 shows the comparison of efficiency of Stirnol engine at different engine RPMs calculated from CFD and experimental work. A good correlation is observed in values apart from high RPM engine conditions. It is because as the engine RPM increases there will be less time for heat addition to Nitinol spring through conduction. In CFD we have added a fix heat addition to Nitinol spring whenever the displacer reaches phase 1 of engine cycle (Fig. 14). High engine RPM would require to make some correction in modelling of this heat addition process.

5. Conclusion

The novel idea of incorporating Nitinol spring in Stirling engine and analyzing its effects on the efficiency and performance of the later through experimentation and computational analysis has been successful in achieving the desired theoretical objectives. Experimentation reveals that Stirnol engine displayed slight improvement in performance as compared to its predecessor Stirling engine. The analysis unveil that this new amalgamation of two fields of science (Stirling engine and Nitinol spring) has revealed positive outcome which can help in extending energy conservation research in the future. Further research in this field is recommended to explore the applicability of the idea of Stirnol engines.

Acknowledgments

I would like to thank the faculty and staff of PNEC, NUST Karachi for their complete support in the fulfillment of this

research. Moreover, the expertise of Pakistan Engineering Vehicles Pvt. Ltd. was utilized in manufacturing the experimental setup.

Conflict of interest

The authors declare that no conflict of interest is associated with the subject of the article.

Author contributions

Humayun Arif contributed towards the idea conception, computation, analysis and Manuscript writing. Muhammad Shafiq contributed through engine modeling in software.

1. G. Walker, Stirling engines. (Oxford, Clarendon Press, 1980).
2. U. R. Singh and A. Kumar, Review on solar Stirling engine: Development and performance, *Thermal Science and Engineering Progress* **8** (2018) 244, https://doi.org/10.1016/j.tsep.2018.08.016.
3. A. C. Ferreira, S. Joao, T. Senhorinha, J. C. Teixeira and S. Azucena Nebra, Assessment of the Stirling engine performance comparing two renewable energy sources: Solar energy and biomass, *Renewable Energy* **154** (2020) 581, https://doi.org/10.1016/j.renene.2020.03.020.
4. S. Zhu, G. Yu, K. Liang, W. Dai and E. Luo, A review of Stirling-engine-based combined heat and power technology. *Applied Energy* **294** (2021) 116965, https://doi.org/10.1016/j.apenergy.2021.116965.
5. B.H. Van Arsdell, Around the world by Stirling engine: environmentally friendly Stirling engines, their applications worldwide and into space, (American Stirling Company, 2003).
6. Badea, Nicolae, ed., Design for micro-combined cooling, heating and power systems: Stirling engines and renewable power systems. (Springer-Verlag London 2015) 137, https://doi.org/10.1007/978-1-4471-6254-4.
7. C. R. Ghanem, N. Gereige Elio, W. S. Bou Nader and J. Mansour Charbel, Stirling system optimization for series hybrid electric vehicles, Proceedings of the Institution of Mechanical Engineers, *Part D: Journal of Automobile Engineering* **236** (2021) 407, https://doi.org/10.1177/09544070211018034.
8. S. H. Omam, Exhaust waste energy recovery using Otto-ATEG-Stirling engine combined cycle, *Applied Thermal Engineering* **183** (2021) 116210, https://doi.org/10.1016/j.applthermaleng.2020.116210.
9. M. A. Abolghasemi, H. Rana, R. Stone, M. Dadd, P. Bailey and K. Lian, Coaxial Stirling pulse tube cryocooler with active displacer, *Cryogenics* **111** (2020) 103143, https://doi.org/10.1016/j.cryogenics.2020.103143.
10. H. Arif, A. Shah, T.A. Ratlamwala, K Kamal and MA. Khan, Effect of Material Change on Stirnol Engine: A Combination of NiTiNOL (Shape Memory Alloy) and Gamma Stirling Engine, *Materials* **16** (2023) 3257, https://doi.org/10.3390/ma16083257.
11. H. Arif, A. Shah, T.A. Ratlamwala, K Kamal and MA. Khan, Stirnol Engine: A combination of Nitinol (shape memory alloy) and Gamma Stirling Engine, *Rev. Mex. Fis.* **69** (2023) 030601, https://doi.org/10.31349/RevMexFis.69.030601.
12. G. Shimoga, T.H. Kim and S.Y. Kim, An intermetallic NiTi-based shape memory coil spring for actuator technologies, *Metals* **11** (2021) 1212, https://doi.org/10.3390/met11081212.
13. Y. Kim, W. Chun and K. Chen, Thermal-flow analysis of a simple LTD (Low-Temperature-Differential) heat engine, *Energies* **10** (2017) 567, https://doi.org/10.3390/en10040567.